doi.org/10.15392/2319-0612.2025.2852
Braz. J. Radiat. Scci., Rio de Janeiro
2025, 13(2A) | 01-17 | e2852
Submitted: 2025-02-03
Accepted: 2025-04-28

Study of dose distribution using Anthropomorphic Phantoms and TL Dosimeters

Vieira[a*], P. H. D. ; Abreu[b], A. E. L. ; Santos[b], Â. M. M. ; Fonseca[a,b], T. C. F.; Meira-Belo[a], L. C.

[a] CDTN - Centro de Desenvolvimento da Tecnologia Nuclear, 30270-901, Belo Horizonte, MG, Brazil
[b] Departamento de Engenharia Nuclear - UFMG, 30270-901, Belo Horizonte, MG, Brazil

*Correspondence: pedro.vieira@cdtn.br

Abstract: This study evaluated dose distribution in radiotherapy protocols using cone beam (100 kVp) and 6 MV beams in two anthropomorphic phantoms: a three-dimensionally (3D) printed skull and the Alderson phantom, with thermoluminescent dosimeters (TL) MTS-N (LiF:Mg,Ti). In the first experiment, 27 TL dosimeters were placed in internal and external regions of the skull, irradiated with a planned dose of 2 Gy in bilateral beams and preceded by a cone beam sequence. Internal dose measurements ranged from 845.92 ± 7.87 mGy to 1041.58 ± 9.69 mGy, representing 40–55% of the planned dose, with the highest absorption in the posterior brain region. Externally, doses corresponded to about 60% of the internal values in the same lateral regions, reflecting the complexity of energy distribution in heterogeneous tissues. In the second experiment, 260 TL dosimeters were distributed in simulated organs of the Alderson phantom, irradiated with a 137Cs beam focused on the spinal cord (166.67 mGy). Organs closest to the beam, such as lungs and heart, received doses significantly higher than the spinal cord (153.21% and 155.61%, respectively), while deeper tissues, such as the spleen and iliacs, presented lower percentages (109.06% and 106.84%). Measurement uncertainties varied, being higher in large organs like the large intestine (24.79%) and superficial tissues like soft tissue (49.96%). The results highlight the efficiency of TL dosimeters in dose validation and underscore the importance of protocol adjustments to address individual patient characteristics, minimizing healthy tissue exposure. The use of anthropomorphic phantoms proved essential for investigating dose distribution heterogeneity, contributing to advancements in radiotherapy precision and safety, with direct impact on treatment efficacy and cancer patients' quality of life.

keywords: dosimetry, radiotherapy, TLD, phantoms;

doi.org/10.15392/2319-0612.2025.2852
Braz. J. Radiat. Scci., Rio de Janeiro
2025, 13(2A) | 01-17 | e2852
Submitted: 2025-02-03
Accepted: 2025-04-28

Estudo da distribuição de doses utilizando Fantomas Antropomórficos e Dosímetros TL

Resumo: Este estudo avaliou a distribuição de doses em protocolos radioterápicos utilizando feixes de cone beam (100 kVp) e 6 MV em dois fantomas antropomórficos: um crânio impresso tridimensionalmente (3D) e o fantoma Alderson, com dosímetros termoluminescentes (TL) MTS-N (LiF:Mg,Ti). No primeiro experimento, 27 dosímetros TL foram posicionados em regiões internas e externas do crânio, irradiado com uma dose planejada de 2 Gy em feixes bilaterais e precedido por uma sequência de cone beam. As doses medidas internamente variaram de 845,92 ± 7,87 mGy a 1041,58 ± 9,69 mGy, representando 40–55% do planejado, com maior absorção na região posterior do cérebro. Externamente, os valores corresponderam a cerca de 60% das doses internas nas mesmas regiões laterais, refletindo a complexidade da distribuição de energia em tecidos heterogêneos. No segundo experimento, 260 dosímetros TL foram distribuídos em órgãos simulados no fantoma Alderson, irradiado com feixe de 137Cs focado na medula espinhal (166,67 mGy). Observou-se que órgãos mais próximos ao feixe, como pulmões e coração, receberam doses significativamente superiores à medula (153,21% e 155,61%, respectivamente), enquanto tecidos profundos, como baço e ilíacos, apresentaram menores percentuais (109,06% e 106,84%). A incerteza varia, sendo maior em órgãos volumosos, como o intestino grosso (24,79%), e em tecidos superficiais, como o tecido mole (49,96%). Os resultados reforçam a eficiência dos dosímetros TL na validação de doses e destacam a importância de ajustes em protocolos radioterápicos para atender às características individuais dos pacientes, minimizando a exposição de tecidos saudáveis. O uso de fantomas antropomórficos mostrou-se essencial para investigar a heterogeneidade da distribuição de doses, contribuindo para avanços na precisão e segurança da radioterapia, com impacto direto na eficácia dos tratamentos e na qualidade de vida dos pacientes oncológicos.

Palavras-chave: dosimetria, radioterapia, tld, fantomas.

1. INTRODUÇÃO

Thermoluminescent dosimeters (TLDs) or TL dosimeters are widely used devices for measuring the amount of ionizing radiation absorbed over time, playing a fundamental role in dose monitoring and control in radiotherapy [1]. These devices operate based on the principle of thermoluminescence, where certain materials, after exposure to radiation, retain energy in defects within their crystalline structure. Subsequently, when these materials are heated, the stored energy is released in the form of light, whose intensity is directly proportional to the absorbed radiation dose [2].

The precision and reliability of TL dosimeters make them an ideal choice for dosimetry in radiotherapy, where it is crucial that prescribed doses are administered with high accuracy to target tissues while minimizing exposure to healthy tissues [1, 3].

In this study, we investigated the dose distribution in different regions of two physical phantoms: a skull phantom and the thoracic region of the Alderson phantom [4]. MTS-N TLDs, made of lithium fluoride doped with magnesium and titanium, were placed in the phantoms, which were irradiated using radiation beam fields of different energies. In the skull phantom, the protocol was designed for an irradiation of 2 Gy to the brain, with dose measurements performed both on the external surface of the brain and on the outer surface of the skull. In the Alderson phantom, the TLDs were positioned inside the thoracic organs to measure the internal dose distribution. The objective of this study was to analyze the dose distribution in the TLDs by calculating uncertainties and measurement errors while comparing the dose readings with the planned doses in the phantoms.

2. MATERIALS AND METHODS

2.1. Experiment with Skull Phantom at Hospital MaterDei in BH

The first experiment followed a brain irradiation radiotherapy protocol. The irradiations were performed using a 6 MV Elekta Versa HD linear accelerator, which was provided by Hospital MaterDei in Belo Horizonte, MG. A total of 27 TL dosimeters and a skull phantom were used in the study. Eighteen TL dosimeters were positioned internally in contact with the brain surface, while nine TL dosimeters were placed on the external surface of the skull, as shown in Figure 1.

Figure 1: Red dots indicate the position of the internal TL dosimeters, with (a) the right lateral surface, (b) the left lateral surface, (c) the posterior surface, (d) the anterior surface, (e) the upper surface, and (f) the lower surface.

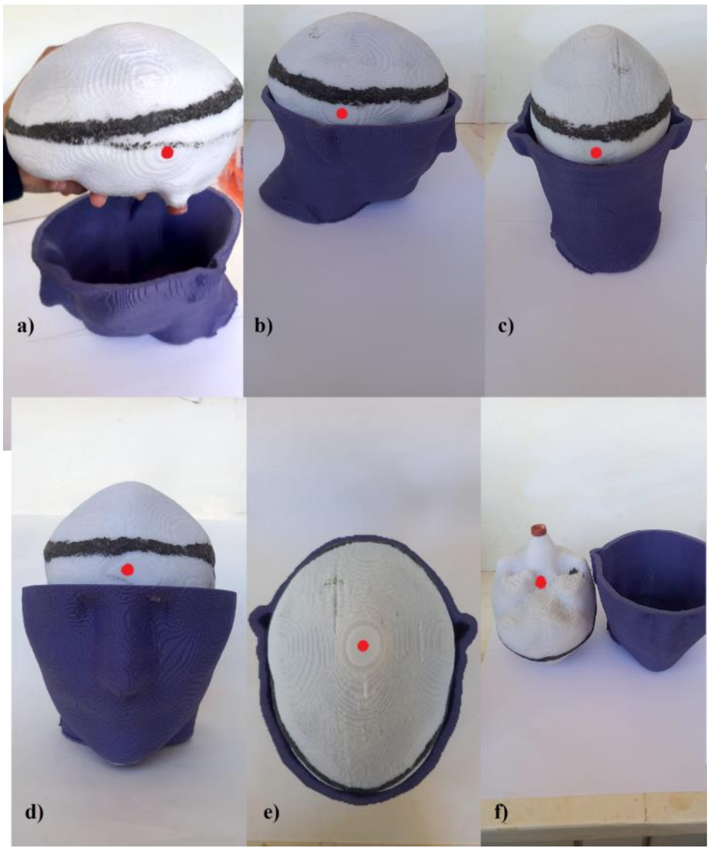

Source: Author

The skull was three-dimensionally (3D) printed by the Monte Carlo Modelling Expert Group (MCMEG) at the Internal Dosimetry Laboratory (LDI/CDTN) and is composed of two main structures: the cranial vault, made of ABS (acrylonitrile butadiene styrene), and the brain, which is hollow and made of PLA (polylactic acid) [5].

The phantom's brain was filled with gel, and the protocol applied two bilateral 6 MV beams, delivering a total dose of 2 Gy. Before applying the 6 MV treatment protocol, the skull underwent a normal treatment positioning verification process. For this purpose, a cone beam was used, operating at 100 kVp, with a dose of 0.5 mGy, as estimated by the treatment planning system (TPS) of the radiotherapy service.

The experiment configuration is presented in Table 1:

1. Internal Distribution of TL Dosimeters:

Table 1: Positioning, quantity, and designation of TL dosimeters in the internal distribution of the skull phantom.

Positioning	Quantity of TLDs	Designation
Upper Internal Surface	3	A1, B1, C1
Right Lateral Internal Surface	3	A2, B2, C2
Left Lateral Internal Surface	3	A3, B3, C3
Posterior Internal Surface	3	A4, B4, C4
Anterior Internal Surface	3	A5, B5, C5
Lower Internal Surface	3	A6, B6, C6

Source: Author

In total, 18 TL dosimeters were fixed internally (in contact with the brain) and remained in place until the completion of the irradiation experiments with cone beam and 6 MV beams.

2.2. External Distribution of TL Dosimeters:

a. First Irradiation: Two TL dosimeters, labeled D1 and D2, were positioned on the left external surface of the skull and irradiated with a 100 kVp cone beam. After irradiation, these TL dosimeters were removed to measure the dose from the cone beam radiation.

b. Second Irradiation: Seven TL dosimeters were positioned externally to measure the dose from the 6 MV beam irradiation:

- Three on the right external surface (D3, D4, D5)
- Three on the left external surface (D6, D7, D8)
- One on the anterior external surface (E8)

Figure 2 illustrates the locations of the external TL dosimeters on the phantom.

Figure 2: Red dots indicate the position of the external TL dosimeters, with (a) the anterior surface, (b) the right lateral surface, and (c) the left lateral surface.

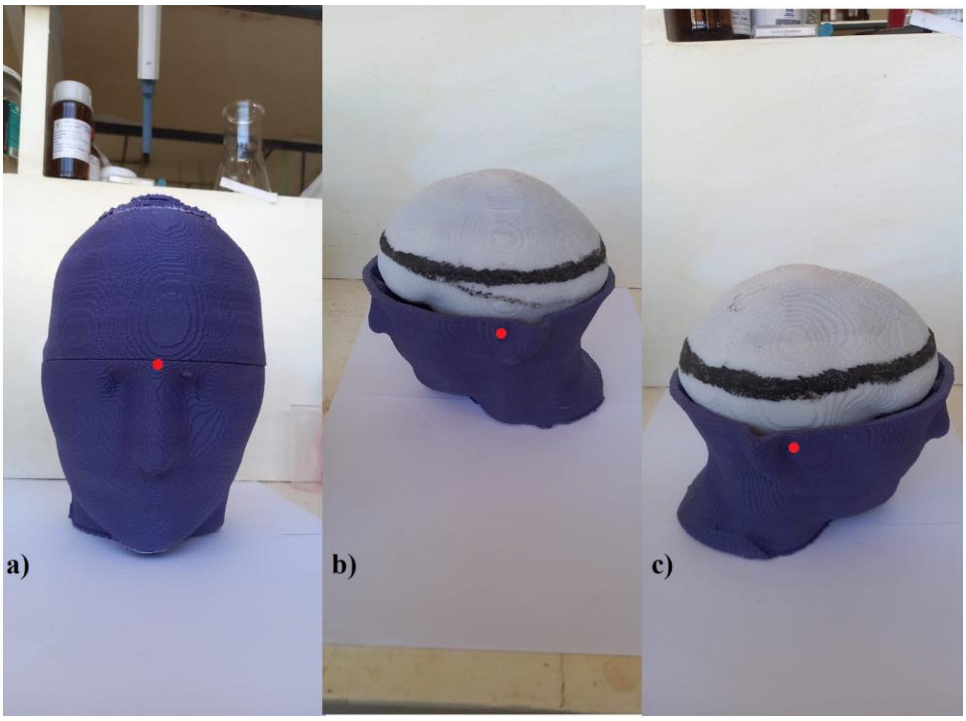

Source: Author

2.3. Irradiation Procedures:

The phantom containing the internal TL dosimeters, D1 and D2, was irradiated with the cone beam. The planning used was for imaging the head and neck protocol, utilizing a cone beam with 100 kVp and an estimated dose of 0.5 mGy according to the TPS. The TL dosimeters, D1 and D2, were removed after irradiation [6].

The phantom was irradiated with the internal TL dosimeters. After that, the external TL dosimeters were added in their positions. The irradiation was performed with a 6MV energy on the accelerator, with two irradiation fields planned, entering from the lateral sides of the phantom, right and left, with a total dose of 2 Gy (2000 mGy), targeting the brain filled with gel.

Figure 3 shows the phantom positioned on the 6 MV linear accelerator table in the radiotherapy service.

Figure 3: External part of the skull phantom with TL dosimeters attached. The black arrow indicates the position of TL dosimeters D1, D2, D6, D7, and D8. The red arrow indicates the position of TL dosimeter E8. TL dosimeters D3, D4, and D5 are positioned on the opposite side of the black arrow.

Source: Author.

2.4. Experiment with Alderson Phantom in the 137Cs Beam at CDTN

The second part of the study was conducted at the Dosimeter Calibration Laboratory at CDTN (LCD/CDTN). For the experiment, 260 thermoluminescent dosimeters were used and placed inside the Alderson phantom to occupy the positions of the organs in the thoracic region as well as the field entrance. Figure 4 shows a slice of the phantom and its organ markings. The torso of the phantom was positioned upright with the field entrance facing forward, approximately 7 meters from the 137Cs irradiator [7]. A planned dose of 166.67 mGy, calculated in the spinal cord region of the phantom, with a total duration of 100,000 seconds (or 27 hours), was recorded. The attenuation of the dose absorbed by the tissues anterior to the spinal cord was not considered in the planned dose [8]. Figure 5 shows the phantom facing the irradiator.

Figure 4: Slice 16 of the phantom with organ markings.

Source: Adapted from [9]

Figure 5: Phantom positioned for irradiation .

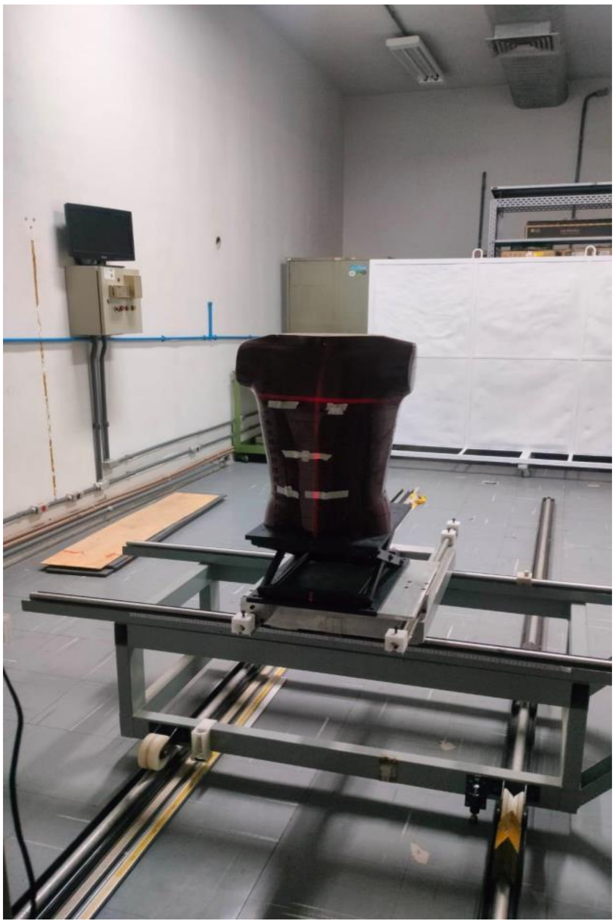

Source: Author

2.5. TLD Readings - SECDOS/CDTN

After irradiating the two phantoms, the TL dosimeters were carefully removed and arranged in a setup where the position of the TL dosimeters could be associated with the region where they were placed in the head and Alderson phantoms.

The TL dosimeters were read using luminescent dosimetry techniques in the SECDOS/CDTN dosimetry laboratory. The RISO TL/OSL DA-20 reader was used, with reading parameters set to a heating rate of 5°C/s, a reading range of 20 to 360°C, under a flow of ultrapure nitrogen. During the reading process, the dosimeters are gradually heated, causing the trapped electrons in the crystal lattice defects to be released and recombine, emitting light proportional to the absorbed radiation dose. This emitted light is detected by a photomultiplier tube, which converts the signal into an electrical response for dose quantification. After reading, the data were analyzed.

Figure 6: The RISO TL/OSL DA-20 reader.

Source: Author

In the experiments with the head phantom, the counting results obtained from the reader for the TLDs were converted into dose and compared with the doses irradiated by the source in the reader with a known dose rate.

The obtained data will be presented in a table along with their respective uncertainties. The uncertainties were obtained from the uncertainty propagation combination of the average between the TL dosimeters and the uncertainties of each dosimeter, obtained after calibration, ensuring greater confidence in the resulting interval. The following equation was used:

$$\sigma_I = \sqrt{\sigma_{\underline{x}}^2 + s} \text{ e } s = \sum_1^N \sigma_{TLD} \quad (1)$$

Where σ_I is the final uncertainty for each position, $\sigma_{\underline{x}}$ is the standard deviation of the absorbed dose in the TLDs, and σ_{TLD} is the uncertainty of each TLD obtained by the reader.

In the Alderson phantom experiment with the 137Cs source, the data were analyzed to obtain the counts in each TLD by the reader and separated by organ in the Alderson phantom. From the counts, the dose ratio was calculated directly by dividing the average counts in the organs (lung, heart, liver, etc.) by the average counts in the spinal cord.

3. RESULTS AND DISCUSSIONS

3.1. Experiment with Head Phantom at MaterDei Hospital in BH

In the experiment with the head phantom irradiated with the 6MV beam and cone beam, with a planned dose of 2 Gy (2000 mGy) for the brain volume, Table 2 was obtained.

Table 2: Values of absorbed dose and their respective uncertainty at each position of the head phantom, with the exposures performed on the TL dosimeters at the position in parentheses.

Position	Absorbed Dose (mGy)	Uncertainty (mGy)
TL dosimeters positioned in the Brain		
Superior of the Brain (cone beam and 6 MV)	845.92	7.87
Inferior of the Brain (cone beam and 6 MV)	867.49	8.07
Right Lateral of the Brain (cone beam and 6 MV)	914.80	8.51
Left Lateral of the Brain (cone beam and 6 MV)	935.05	8.69
Posterior of the Brain (cone beam and 6 MV)	1041.58	9.69
Anterior of the Brain (cone beam and 6 MV)	898.03	8.31
TL dosimeters positioned in the Skull		
Left External of the Skull (cone beam)	1.12	2.55
Left External of the Skull (cone beam and 6 MV)	557.36	5.47
Right External of the Skull (cone beam and 6 MV)	549.67	5.36
Frontal External of the Skull (cone beam and 6 MV)	206.46	4.97

Source: Author

3.2. Irradiation of the Brain with the 6MV Beam and a Dose of 2 Gy

The dose calculated by the TPS (Treatment Planning System) of the radiotherapy service for the 6 MV beam to the brain (target organ) was 2 Gy (2000 mGy), or 1 Gy for each lateral, with a maximum possible variation of 5%. The results of the absorbed doses in the TL dosimeters, positioned inside the skull and outside the brain, indicated that the measured dose was lower, between 40% and 55% (between 845.92 mGy ± 7.87 mGy and 1041.58 mGy ± 9.69 mGy), than the planned value for the target. These values were expected, as the brain was the target organ and the total dose should have been within this organ. The highest doses in the phantom irradiation were recorded in the posterior region of the brain, even though the field entry was from the lateral sides. The posterior face received values close to 55% (1041.58 mGy ± 9.69 mGy) of the planned dose for the target in the brain. The external TL dosimeters, positioned on the right and left sides, in the radiotherapy protocol with the brain as the target, received doses ranging from 25% to 40% of the dose in the target. The field entry was made from the right and left lateral sides. The doses measured in the external TL dosimeters corresponded to approximately 60% of the doses in the internal TL dosimeters located on the same lateral faces (549.67 mGy ± 5.36 mGy and 557.36 mGy ± 5.37 mGy), due to the higher dose contribution from the field entry on the same side.

3.3. Cone beam

The first irradiation with the cone beam on the head resulted in doses of approximately 1.12 mGy with 227% uncertainty, while the dose estimated by the TPS was 0.5 mGy, without an associated uncertainty, as it is merely an estimation (for cone beam imaging, the TPS is designed to plan the image acquisition rather than a specific dose delivery; therefore, the reported dose is merely a byproduct of the imaging process and not an intended treatment dose). The high uncertainty of 227% in the cone beam measurements is likely due to the low dose levels involved, which can lead to greater variability in TL dosimeter readings, as well as potential signal fluctuations and background noise interference in the dosimetry process. This indicates a low dose delivered during cone beam imaging for the head and neck region. Figure 6 presents the image obtained from the head phantom using the cone beam.

Figure 7: Image generated in the cone beam of the head phantom in a frontal plane.

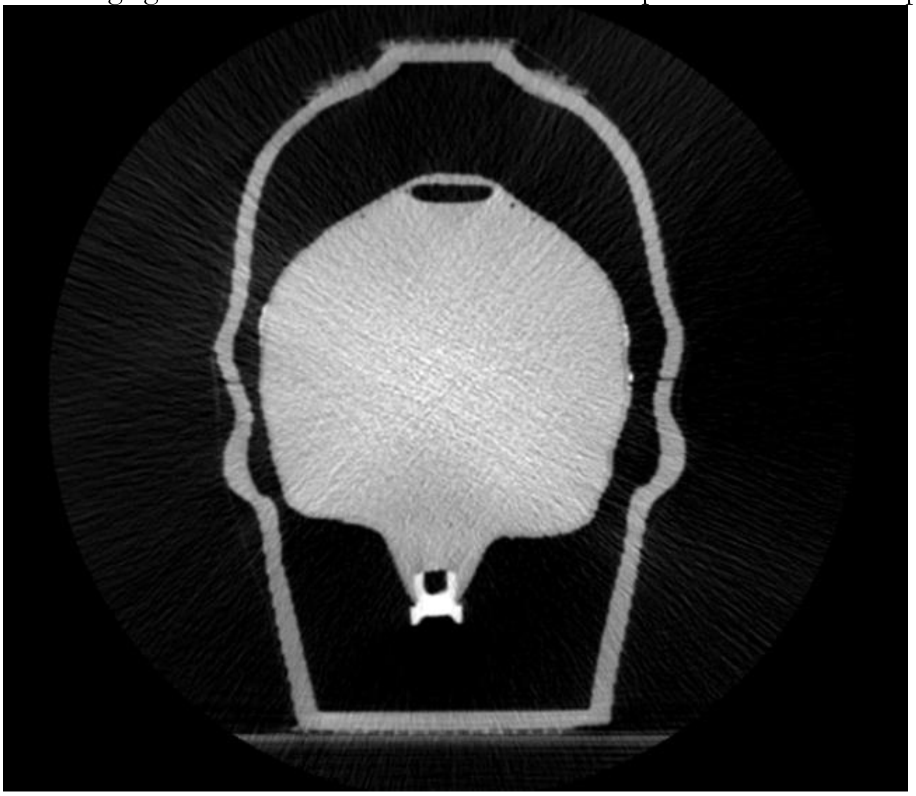

Source: Author

3.4. Experiment with Alderson Phantom in the 137Cs Beam at CDTN

For the Alderson phantom experiment, in which a dose of 166.67 mGy was irradiated to the spinal cord by a 137Cs source, the dose ratio between the average in the organs and the average in the spinal cord was found in Table 3.

Table 3: Dose Ratio between the Average in the Spinal Cord and the Average in the Organs in Percentage Values.

Organs	Dose/Dose (%)	Uncertainty (%)
Lung	153.21%	18.13%
Heart	155.61%	13.51%

Organs	Dose/Dose (%)	Uncertainty (%)
Liver	172.45%	24.79%
Kidneys	120.55%	7.46%
Esophagus	143.46%	22.10%
Spleen	109.06%	4.98%
Large Intestine	164.73%	3.53%
Small Intestine	185.26%	12.53%
Soft Tissue	124.23%	49.96%
Iliacs	106.84%	31.37%

Source: Author

The irradiation of the Alderson phantom demonstrated a significant variation in doses among the analyzed organs, highlighting the influence of proximity to the field entrance and tissue attenuation. The lungs and heart showed higher doses compared to the spinal cord, with values of 153.21% and 155.61%, respectively.

In contrast, deeper organs or those with higher attenuation, such as the spleen and iliacs, showed doses of 109.06% and 106.84%, respectively. This behavior reflects the expected distribution in an anthropomorphic phantom, where tissue density and geometry directly influence the distribution of absorbed energy.

Moreover, the uncertainty in the measurements was greater in larger volume organs, such as the large intestine, which had an uncertainty of 24.79%. This is due to the heterogeneous dose distribution within the organ. For soft tissue, the highest overall uncertainty was observed, reaching 49.96%, possibly due to its low density and its location near the phantom's surface.

The results strongly emphasize the crucial importance of carefully adjusting protocols for specific organs, taking into account tissue characteristics and attenuation. This optimization is essential to enhance the accuracy of radiotherapy treatments, ensuring more precise dose delivery and improving treatment effectiveness.

4. CONCLUSION

The results of this study demonstrate the efficiency of TL dosimeters in measuring and validating dose distribution in radiotherapy protocols. The application of anthropomorphic phantoms, such as the head phantom and the Alderson phantom, proved essential for understanding dose variations in simulated organs and tissues, allowing for more precise adjustments in treatment plans.

The head phantom allowed for the identification of the heterogeneous distribution of internal and external doses, highlighting the relevance of beam calibration. The Alderson phantom, on the other hand, emphasized the influence of tissue density and attenuation on absorbed doses, especially in organs close to the surface.

The differences observed between the planned and measured doses highlight the need for continuous monitoring during the execution of radiotherapy protocols, ensuring that the predicted doses are effectively delivered to the target tissues.

ACKNOWLEDGMENT

The following Brazilian institutions support this research project: the Fundação de Amparo à Pesquisa do Estado de Minas Gerais (FAPEMIG), the Conselho Nacional de Desenvolvimento Científico e Tecnológico (CNPq). We also thank the FAPEMIG Project: Rede Mineira de Pesquisa Translational em Oncologia RED00059-23, INCT. INAIS: Nuclear Instrumentation and Applications in Industry and Health, Hospital Mater Dei for providing the radiotherapy service for the work, and the Centro de Desenvolvimento da Tecnologia Nuclear - CDTN.

CONFLICT OF INTEREST

All authors declare that they have no conflicts of interest.

REFERENCES

[1] GIBBONS, J. P. Khan's The Physics of Radiation Therapy. Lippincott Williams & Wilkins, 2014.

[2] HOROWITZ, Y. S. Thermoluminescence and thermoluminescent dosimetry. Nuclear Technology, v. 90, n. 1, p. 75-93, 1990. DOI: 10.13182/NT90-A34428.

[3] McKEEVER, S. W. S. Thermoluminescence of Solids. Cambridge University Press, 1985. DOI: 10.1017/CBO9780511564991.

[4] RSD. Anatomy. 2022. Disponível em: https://rsdphantoms.com/product/the-alderson-radiation-therapy-phantom/. Acesso em: 14 jan. 2025.

[5] VITAL, K. D.; MENDES, B. M.; DE SOUSA LACERDA, M. A.; DA SILVA, T. A.; FONSECA, T. C. F. Development of a physical head phantom using a solid brain equivalent tissue for the calibration of the 18F-FDG internal monitoring system. Radiation Physics and Chemistry, v. 155, p. 56-61, 2019.

[6] HVID, C. A.; ELSTRØM, U. V.; JENSEN, K.; GRAU, C. Cone-beam computed tomography (CBCT) for adaptive image-guided head and neck radiation therapy. Acta Oncologica, v. 57, n. 4, p. 552–556, 2017. DOI: 10.1080/0284186X.2017.1398414.

[7] OMOJOLA, A. D. et al. Calibration of MTS-N (LiF: Mg, Ti) chips using cesium-137 source at low doses for personnel dosimetry in diagnostic radiology. Radiation Protection and Environment, v. 43, n. 2, p. 108, 2020.

[8] INTERNATIONAL COMMISSION ON RADIATION UNITS AND MEASUREMENTS (ICRU). Report 85: Fundamental Quantities and Units for Ionizing Radiation. ICRU Publications, 2010.

[9] REYNALDO, T. A. D. S. S. R. A dosimetria de pacientes em exames em raios X: implantação da capacidade metrológica em Minas Gerais. [S.l.]: CNEN, 2009.

LICENSE